Roughness-induced wetting

Roland R. Netz* and David Andelman
School of Physics and Astronomy, Raymond and Beverly Sackler Faculty of Exact Sciences, Tel Aviv University, Ramat Aviv 69978, Tel Aviv, Israel

(Received 8 February 1996; revised manuscript received 29 July 1996)

We investigate theoretically the possibility of a wetting transition induced by geometric roughness of a solid substrate for the case where the flat substrate does not show a wetting layer. Our approach makes use of a closed-form expression that relates the interaction between two sinusoidally modulated interfaces to the interaction between two flat interfaces. Within the harmonic approximation, we find that roughness-induced wetting is indeed possible if the substrate roughness, quantified by the substrate surface area, exceeds a certain threshold. In addition, the molecular interactions between the substrate and the wetting substance have to satisfy several conditions. These results are expressed in terms of a lower bound on the wetting potential for a flat substrate in order for roughness-induced wetting to occur. This lower bound has the following properties. A minimum is present at zero or very small separation between the two interfaces, as characteristic for the nonwetting situation in the flat case. Most importantly, the wetting potential needs to have a pronounced maximum at a separation comparable to the amplitude of the substrate roughness. These findings are in agreement with the experimental observation of roughness-induced surface premelting at a glass-ice interface as well as the calculation of the dispersion interaction for the corresponding glass-water-ice system. [S1063-651X(97)07101-8]

PACS number(s): 68.45.Gd, 68.15.+e, 68.35.−p

I. INTRODUCTION

The phenomenon of wetting has been the subject of intense attention and a fairly good understanding of the basic concepts and mechanisms has emerged [1–3]. In the simplest case, a solid inert surface is put in contact with an undersaturated vapor of a second substance. Typically, a molecularly thick liquidlike film will form on the substrate surface due to favorable molecular interactions. The liquid film is in equilibrium with its undersaturated vapor, thus giving rise to a second interface (the emerging liquid-vapor interface), referred to hereafter as the liquid interface. Depending on the detailed molecular interactions between all three phases and the resulting interfacial energies, the liquid film can either grow to macroscopic thickness or remain finite as coexistence between the liquid and its vapor is approached. The first situation corresponds to *complete wetting* with a diverging film thickness, the second case is called *incomplete* or *partial wetting*.

Two other, closely related situations are possible. (i) The liquid layer (e.g., water) on the inert substrate can be in equilibrium with its solid phase (ice) at temperatures below the melting point. In this case the vapor is replaced by a solid and the appearance of a thin liquid layer between the substrate and the solid phase indicates interfacial premelting. Note that the third phase (the ice) is entirely different from the solid substrate. (ii) The substrate itself can be a solid in equilibrium with its vapor phase. Here the formation of a thin liquid layer as three-phase coexistence is approached corresponds to surface premelting [4]. The phenomenological description of these scenarios does not differ from the wetting situation, and one finds the analogous phenomena corresponding to partial and complete wetting.

In early theoretical studies, the solid substrate was assumed to be flat and homogeneous. However, in most experimental and technological situations the substrate is both rough and inhomogeneous. For complete wetting upon approaching coexistence, where the liquid forms a thin and continuous film, the influence of substrate roughness and chemical disorder has recently been investigated theoretically [5–9] and experimentally [10–13] in great detail. It was found that heterogeneity and roughness of the solid substrate in conjunction with long-range van der Waals interactions cause equilibrium undulations of the liquid film surface. Surface tension, on the other hand, acts as a damping mechanism that reduces the amplitude of undulations for thicker films. The theoretical results [5,8] were verified recently in small-angle x-ray scattering [11–13].

Yet another realization of the wetting phenomenon is obtained if a *nonvolatile* liquid is spread on a solid surface; in technological applications, the liquid might be a paint or a lubricant. In this case, the liquid is neither in phase equilibrium with the solid substrate nor with the gaseous phase and the total amount of liquid on the substrate is a conserved quantity [1]. In the complete wetting situation, the liquid forms a continuous film on the substrate; in the partial or incomplete wetting case, the liquid forms droplets with the contact angle being determined by the interfacial energies between the three phases meeting at the contact line [14]. Roughness of the substrate has been shown to cause contact angle hysteresis for advancing and receding contact lines [1,15].

Much work was specifically concerned with the interfacial and surface premelting properties of ice, due to its atmospheric and environmental consequences [16]. Surface premelting of ice has been observed by a variety of

*Present address: Max-Planck-Institut für Kolloid- und Grenzflächenforschung, Kantstr.55, 14513 Teltow-Seehof, Germany.

experimental techniques [17–19] and it is now believed that complete surface premelting (i.e., macroscopic growth of the surface liquid layer as the melting temperature is approached) occurs only for some orientations of the crystal surface and only if the vapor phase is diluted with air [20]. Interfacial premelting of ice, giving rise to the low sliding friction of ice, has been deduced from wire regelation at low temperature [21] and from viscosity measurements between surfaces of ice and quartz [22]; it also forms the basis for frost heave in frozen soils [23]. Complete interfacial premelting between ice crystals and a glass substrate was detected by ellipsometry [24,25]. The geometric structure of the glass surface was shown to play a vital role in this premelting phenomenon; in a series of experiments, the surface has been roughened by exposition to fluoric acid for different amounts of time, leading to surfaces with varying characteristic height-fluctuation amplitudes and wavelengths [25]. For flat glass substrates the premelting was shown to be incomplete, while complete premelting was exhibited for glass substrates with a threshold amount of microroughness [25].

The latter experimental observation motivated us to explore theoretically the possibility of a *roughness-induced* complete wetting or premelting transition. This describes the situation in which the *flat* substrate, for a given temperature, is not covered with a macroscopic liquid layer as coexistence is approached (corresponding to partial wetting), but, at the same temperature, is completely wet if the roughness of the substrate exceeds a certain threshold (in what follows we will use the wetting terminology both for the phenomena of premelting and wetting). In this paper we critically examine the conditions under which such a phenomenon can occur. As a result, roughness-induced wetting is indeed possible if the involved materials have the following properties: (i) The tension of the substrate-vapor interface has to be larger than that of the substrate-liquid interface, (ii) the surface area increase of the solid substrate due to its roughness has to exceed a certain threshold, which depends on the interfacial tensions of all three phases [25], and (iii) the effective interaction between the two interfaces bounding the liquid layer for the flat case has to have a maximum for separations of about the amplitude of the substrate roughness. We also find that roughness-induced wetting is most likely to occur when the substrate roughness just exceeds a certain threshold value and will disappear for very large amplitudes of the roughness.

The outline of this paper is as follows. In Sec. II we introduce the model and review some nomenclature for the case of a flat substrate. In Sec. III we extend the analysis to the case of a rough substrate. We first give necessary and rather general conditions under which roughness-induced wetting is possible. Using a formula that describes the van der Waals interaction between two sinusoidal surfaces, we then construct a sufficient condition for roughness-induced wetting in the form of a lower bound for the interaction between two flat interfaces. Finally, Sec. IV contains the discussion.

II. FLAT SUBSTRATE

Consider the situation as illustrated in Fig. 1, where a thin liquid film intrudes in between an inert solid surface and a

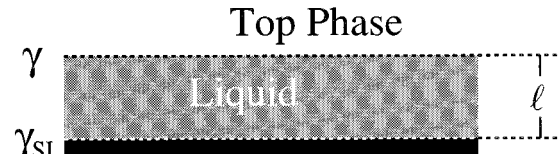

FIG. 1. Schematic view of a flat substrate: A liquid layer of thickness l intrudes between the inert substrate and the top phase, which can be either the vapor or the solid in chemical equilibrium with the liquid, corresponding to wetting or interfacial premelting, respectively. The liquid-substrate and liquid-top phase interfacial energies are denoted by γ_{SL} and γ, respectively.

top phase. The top phase can be either a vapor or a solid in thermodynamic equilibrium with the liquid film. The solid substrate, on the other hand, is completely frozen and far from its melting point. In this section, we will review results for an ideal solid substrate, namely, molecularly flat and homogeneous. Using the convention of labeling all physical quantities with a *zero* subscript for the flat case, the free energy per unit area can be written as

$$\mathcal{F}^0(l)=\gamma_{SL}+\gamma+P^0(l)+\mu l, \tag{1}$$

where γ_{SL} denotes the solid-liquid interfacial tension and γ denotes the interfacial tension between the liquid and the top phase. The parameter μ is the chemical potential difference between the liquid and top phases. Alternatively, it could also correspond to a Lagrange multiplier controlling the film thickness for nonvolatile liquids with conserved total volume. The potential $P^0(l)$ represents the interaction per unit area between the two flat interfaces with a separation of l and can be viewed as a thickness-dependent correction to the interfacial energies, depending both on the short and long-ranged parts of the molecular interactions [26].

In the simplest approach, assuming pairwise additive interactions between molecules and uniform densities in all coexisting phases, $P^0(l)$ can be expressed as

$$P^0(l)\equiv\int_l^\infty dz\int d^2\boldsymbol{\rho}\int_{-\infty}^0 dz'\,w(\boldsymbol{\rho},z-z'), \tag{2}$$

where $w(\boldsymbol{\rho},z)$ corresponds to the local interaction energy difference per unit volume squared between the solid and the third phase. Dropping some constant terms, it can be written as

$$w(\mathbf{r})=n_L^2U_{LL}(\mathbf{r})-n_Ln_SU_{LS}(\mathbf{r})-n_Ln_TU_{LT}(\mathbf{r})+n_Tn_SU_{TS}(\mathbf{r}). \tag{3}$$

Here $U_{ij}(\mathbf{r})$ are the pair interactions between molecules and the n_i are the particle number densities for each phase, where i and j are any of the relevant phases: solid (S), liquid (L), and top (T) [5]. In a more realistic approach, one calculates Eq. (2) directly using the Lifshitz continuum theory of dispersion interactions [27].

In general, $P^0(l)$ is expected to vanish for $l\to\infty$ as the two interfaces become decoupled and approaches a finite value for $l\to 0$ [29]. One therefore defines

$$P^0(l)=\begin{cases}0 & \text{for} \quad l\to\infty\\ S & \text{for} \quad l\to 0,\end{cases} \tag{4}$$

where S is traditionally called the *spreading coefficient* and is given by

$$S\equiv\gamma_{ST}-\gamma_{SL}-\gamma. \tag{5}$$

The above definition leads to $\mathcal{F}^0(0)=\gamma_{ST}$, just as one would expect: In the absence of any liquid, the total free energy is given by the interfacial tension between the solid and the top phase [30]. On the other hand, for an infinite layer of liquid coexisting with the top phase, one finds $\mathcal{F}^0(\infty)=\gamma_{SL}+\gamma$ for $\mu=0$, i.e., the two interfaces bounding the liquid do not interact and the total free energy is given by the sum of the two interfacial energies alone. One can notice that positive values of $S=P^0(0)-P^0(\infty)=\mathcal{F}^0(0)-\mathcal{F}^0(\infty)$ correspond to a situation where an infinite liquid layer is energetically preferred over a vanishing liquid layer. Indeed, neglecting the possibility of additional minima of $P^0(l)$ at intermediate values of l, positive and negative values of S correspond to wetting and nonwetting cases, respectively. On the other hand, in the case of a nonvanishing chemical potential μ, the minimum of the free energy will always be at finite film thickness, even for positive spreading coefficient S [31].

In the following, we will be exclusively concerned with the nonwetting case, i.e., $S<0$. It will be convenient to modify the definition of the free energy slightly and to take the infinitely thick liquid layer as the reference state. The free-energy difference, defined by $\Delta\mathcal{F}^0(l)\equiv\mathcal{F}^0(l)-\mathcal{F}^0(\infty)$ and in the case of vanishing chemical potential $\mu=0$, is given by

$$\Delta\mathcal{F}^0(l)=P^0(l), \tag{6}$$

with the limiting values

$$\Delta\mathcal{F}^0(l)=\begin{cases}0 & \text{for} \quad l\to\infty\\ S & \text{for} \quad l\to 0.\end{cases} \tag{7}$$

Clearly, a wetting situation is realized if $\Delta\mathcal{F}^0(l)>0$ holds for all $l<\infty$.

III. ROUGH SUBSTRATE

We introduce now the necessary framework to describe wetting on geometrically rough solids [32]. The free energy per unit projected area for a liquid film on a rough solid substrate (see Fig. 2) can be written as

$$\mathcal{F}(\boldsymbol{\rho},[\zeta_L])=\sqrt{1+[\nabla\zeta_S(\boldsymbol{\rho})]^2}\,\gamma_{SL}+\sqrt{1+[\nabla\zeta_L(\boldsymbol{\rho})]^2}\,\gamma +P(\boldsymbol{\rho},[\zeta_L])+\mu[\zeta_L(\boldsymbol{\rho})-\zeta_S(\boldsymbol{\rho})]. \tag{8}$$

The solid and liquid surfaces are parametrized by $\zeta_S(\boldsymbol{\rho})$ and $\zeta_L(\boldsymbol{\rho})$, respectively, where $\boldsymbol{\rho}$ is a two-dimensional vector in a reference plane. The interaction term $P(\boldsymbol{\rho},[\zeta_L])$ is a generalization of $P^0(l)$ [Eq. (2)] and is defined by

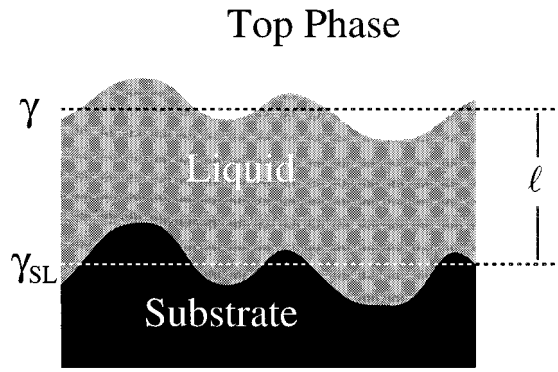

FIG. 2. Liquid film on a rough substrate: For thin mean film thickness l, defined by the averaged local separation between the two interfaces, the liquid interface follows the substrate corrugations.

$$P(\boldsymbol{\rho},[\zeta_L])=\int_{\zeta_L(\boldsymbol{\rho})}^{\infty}dz\int d^2\boldsymbol{\rho}'\int_{-\infty}^{\zeta_S(\boldsymbol{\rho}+\boldsymbol{\rho}')}dz'\,w(\boldsymbol{\rho}',z-z'). \tag{9}$$

Note that expression (9) is a local function of the liquid profile $\zeta_L(\boldsymbol{\rho})$, but a nonlocal functional of the rough solid surface $\zeta_S(\boldsymbol{\rho})$. For the discussion of wetting behavior it is useful to average over the in-plane coordinate $\boldsymbol{\rho}$, by which we obtain the effective wetting free energy

$$\overline{\mathcal{F}}(l,[\zeta_L])\equiv\langle\mathcal{F}(\boldsymbol{\rho},[\zeta_L])\rangle_{\boldsymbol{\rho}}, \tag{10}$$

where we explicitly pulled out the dependence on the average film thickness

$$l\equiv\langle\zeta_L(\boldsymbol{\rho})-\zeta_S(\boldsymbol{\rho})\rangle_{\boldsymbol{\rho}}. \tag{11}$$

This parameter measures the average distance between the two interfaces. The effective free energy (10) can be written as

$$\overline{\mathcal{F}}(l,[\zeta_L])=\alpha_S\gamma_{SL}+\alpha_L(l,[\zeta_L])\,\gamma+\overline{P}(l,[\zeta_L])+\mu l. \tag{12}$$

In analogy to Eq. (10), the effective wetting potential $\overline{P}(l,[\zeta_L])$ is obtained from Eq. (9) by averaging over the in-plane coordinate

$$\overline{P}(l,[\zeta_L])\equiv\langle P(\boldsymbol{\rho},[\zeta_L])\rangle_{\boldsymbol{\rho}}. \tag{13}$$

The parameters α_S and $\alpha_L(l,[\zeta_L])$ measure the ratios between the actual and projected areas of the substrate surface and liquid interface, respectively, and are defined by

$$\alpha_S\equiv\langle\sqrt{1+[\nabla\zeta_S(\boldsymbol{\rho})]^2}\rangle_{\boldsymbol{\rho}}, \tag{14}$$

$$\alpha_L(l,[\zeta_L])\equiv\langle\sqrt{1+[\nabla\zeta_L(\boldsymbol{\rho})]^2}\rangle_{\boldsymbol{\rho}}. \tag{15}$$

On the mean-field level considered in this paper, one can take the liquid interface to assume a fixed profile $\zeta_L^*(\boldsymbol{\rho})$ so as to minimize the free-energy expression (12). By construction of the functional (12), this amounts to a constrained minimi-

zation of the free energy for a fixed average film thickness l. This yields the minimized free energy, denoted by $\overline{\mathcal{F}}^*$, as a function of l,

$$\overline{\mathcal{F}}^*(l) \equiv \min_{[\zeta_L]} \overline{\mathcal{F}}(l,[\zeta_L]) = \overline{\mathcal{F}}(l,[\zeta_L^*]). \tag{16}$$

The area ratio of the optimal liquid interface ζ_L^* has the limiting values

$$\alpha_L^*(l) \equiv \alpha_L(l,[\zeta_L^*]) = \begin{cases} \alpha_S & \text{for} \quad l \to 0 \\ 1 & \text{for} \quad l \to \infty \end{cases} \tag{17}$$

since a very thin liquid layer follows the solid substrate roughness completely, whereas a thick enough layer will be essentially flat (neglecting thermal capillary roughness). Just as for the flat case, $\overline{P}^*(l) \equiv \overline{P}(l,[\zeta_L^*])$ is expected to vanish for infinitely separated interfaces, i.e., $\overline{P}^*(\infty)=0$. The interaction at contact (for $l=0$) is, to a first approximation, given by the interaction of the flat case times the surface area ratio of the rough solid surface, i.e., $\overline{P}^*(0) \approx \alpha_S P^0(0) = \alpha_S S$ [33]. Defining the free-energy difference by $\Delta\overline{\mathcal{F}}(l,[\zeta_L]) \equiv \overline{\mathcal{F}}(l,[\zeta_L]) - \overline{\mathcal{F}}^*(\infty)$, for which we set $\mu=0$ (the introduction of a nonzero chemical potential is straightforward and will be treated separately in Sec. III C), one finds

$$\Delta\overline{\mathcal{F}}(l,[\zeta_L]) = \{\alpha_L(l,[\zeta_L]) - 1\}\gamma + \overline{P}(l,[\zeta_L]). \tag{18}$$

The limiting values of the free energy $\Delta\overline{\mathcal{F}}^*(l)$ (obtained by minimizing with respect to the liquid interface profile ζ_L) are given by

$$\Delta\overline{\mathcal{F}}^*(l) = \begin{cases} \alpha_S(\gamma_{ST} - \gamma_{SL}) - \gamma & \text{for} \quad l \to 0 \\ 0 & \text{for} \quad l \to \infty. \end{cases} \tag{19}$$

It is instructive to define the effective spreading coefficient $S_{\text{eff}} \equiv \Delta\overline{\mathcal{F}}^*(0)$, which can be written as

$$S_{\text{eff}} = \alpha_S(\gamma_{ST} - \gamma_{SL}) - \gamma = (\alpha_S - 1)\gamma + \alpha_S S. \tag{20}$$

From Eq. (2) it follows that the effective spreading coefficient is always larger than the bare spreading coefficient S since $\gamma > 0$ and $\alpha_S > 1$. The substrate area ratio can be expressed in terms of the spreading coefficients and the liquid interfacial tension as

$$\alpha_S = \frac{S_{\text{eff}} + \gamma}{S + \gamma}. \tag{21}$$

A. Definition of roughness-induced wetting

With the definitions of the previous sections we are now able to clearly define the subject and purpose of the present work. As already stated in the Introduction, we are concerned with the case where the flat substrate is not wet, i.e., the free-energy difference $\Delta\mathcal{F}^0(l)$ for the flat case [Eq. (6)], is negative for some finite value of l. The central question is, under which conditions will the rough substrate be wet, i.e., under which conditions does

$$\Delta\overline{\mathcal{F}}^*(l) > 0 \tag{22}$$

hold for all finite film thicknesses $l < \infty$? The answer of course imposes conditions both on the magnitude of substrate roughness (measured by α_S) and on the interactions between the coexisting phases, i.e., on the molecular interaction $w(\boldsymbol{\rho},z)$, which enters the calculation of the wetting potential in Eq. (9).

In Sec. III B we give two rather general necessary conditions for roughness-induced wetting, which hold at very small wetting-layer thickness and rather large layer thickness (as compared to the substrate roughness amplitude), respectively. For the intermediate film thickness, we derive a sufficient condition in Sec. III C.

B. Necessary conditions for roughness-induced wetting

1. Necessary condition for vanishing film thickness

The necessary condition for a roughness-induced wetting transition that corresponds to Eq. (22) for vanishing film thickness ($l \to 0$) follows from Eqs. (19) and (20). It can be written as $S_{\text{eff}} > 0$, which, together with the nonwetting condition for the flat case ($S<0$), leads to the inequalities [25]

$$\gamma_{ST} - \gamma_{SL} < \gamma < \alpha_S(\gamma_{ST} - \gamma_{SL}). \tag{23}$$

These inequalities can only be satisfied if $\gamma_{ST} > \gamma_{SL}$ holds, since $\alpha_S \geqslant 1$ by definition. From Eq. (5) one then also obtains that $\gamma > -S$ has to hold. Equation (23) also imposes a lower bound on the substrate surface ratio α_S,

$$\alpha_S > \frac{1}{1 + S/\gamma}. \tag{24}$$

Clearly, the conditions (23) and (24), although necessary, are not sufficient for wetting, since the free energy $\Delta\overline{\mathcal{F}}^*(l)$ can develop a minimum at finite separation l. The conditions (23) and (24) simply correspond to a situation where the $l \to \infty$ thick liquid layer has a lower interfacial energy than a film of vanishing thickness $l \to 0$.

2. Harmonic approximation

We now introduce the harmonic approximation, which we will adhere to in the remainder of this paper. Consider a corrugated solid surface, chosen to have sinusoidal undulations along one direction ρ_1 of the two-dimensional reference plane (ρ_1,ρ_2) with amplitude h_S and wave number q,

$$\zeta_S(\boldsymbol{\rho}) \equiv h_S \sin(q\rho_1). \tag{25}$$

The liquid profile is approximately (within linear-response theory) characterized by the same q-mode undulation with a different amplitude h_L, vertically displaced by the film thickness l,

$$\zeta_L(\boldsymbol{\rho}) \equiv h_L \sin(q\rho_1) + l. \tag{26}$$

This geometry is depicted in Fig. 3. To linear order, there is also no phase shift between the two surfaces. In the following, the amplitude h_S is assumed to be positive, with no loss of generality. The interfaces cannot penetrate each other,

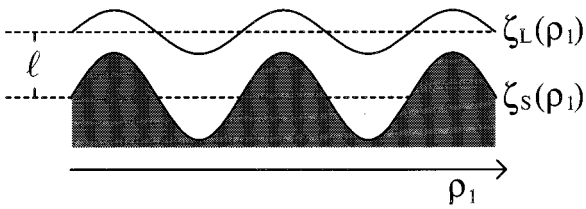

FIG. 3. Simplified geometry in the single q-mode approximation, with the substrate surface parameterized by $\zeta_S(\rho_1)$ and the liquid interface parametrized by $\zeta_L(\rho_1)$, shown along the direction parallel to the wave vector of the sinusoidal profile. The mean separation l corresponds to the distance between the mean positions of the interfaces, denoted by broken lines.

constituting the *noncrossing condition*, which can be written as $\zeta_L(\boldsymbol{\rho}) \geqslant \zeta_S(\boldsymbol{\rho})$, valid at any point $\boldsymbol{\rho}$. This leads to the constraints

$$h_S - l \leqslant h_L \leqslant l + h_S. \tag{27}$$

Expanding the expressions for the interfacial ratios α_S and α_L [Eqs. (14) and (15)] and keeping only terms up to quadratic order in the amplitudes h_L and h_S leads to the following expressions for the area ratios:

$$\alpha_S = 1 + \frac{1}{4} h_S^2 q^2 + \mathcal{O}((h_S q)^4), \tag{28}$$

$$\alpha_L = 1 + \frac{1}{4} h_L^2 q^2 + \mathcal{O}((h_L q)^4), \tag{29}$$

which are expected to be good approximations for weakly corrugated interfaces (as long as $h_S q \ll 1$ and $h_L q \ll 1$). The necessary condition for roughness-induced wetting at vanishing film thickness (24) becomes

$$\alpha_S \simeq 1 + \frac{1}{4} h_S^2 q^2 > \frac{1}{1 + S/\gamma}. \tag{30}$$

We now identify two different physical regimes. For $\gamma \gtrsim -S$, defining the *interaction-dominated regime*, the necessary condition for wetting leads to $h_S q \gg 1$ and the expansion in terms of hq breaks down. Here the solid roughness has to be quite pronounced and the behavior of the liquid interface turns out to be mostly dominated by the short-ranged part of the molecular interaction. For $\gamma \gg -S$, defining the *tension-dominated regime*, condition (30) can be fulfilled even for small solid roughness ($h_S q \ll 1$); here the liquid interface is dominated by its surface tension. It is the tension-dominated regime where the approximations leading to Eqs. (28) and (29) and other simplifications made in the remainder of this paper are valid; this is also the regime of most practical interest, since values for $h_S q$ characterizing rough surfaces in experiments are typically quite small [34].

3. Necessary condition for thick films

An additional necessary condition for wetting is $\overline{P^*}(l) > 0$, valid for average film thicknesses approximately larger than the corrugation amplitude, $l \gtrsim h_S$. This condition can be obtained in the following way. Suppose we have a flat liquid interface, i.e., $\alpha_L = 1$. Then the first term in Eq. (18) vanishes, and in order for the minimized free-energy difference $\Delta\overline{\mathcal{F}^*}(l)$ to be positive we have to require that $\overline{P^*}(l) > 0$. Clearly, a flat liquid interface is possible only for a liquid layer thickness that is larger than the amplitude of the solid roughness, otherwise the two interfaces sterically interact. Figure 4 schematically depicts the limiting case $l \approx h_S$ with the flat liquid interface just touching the solid substrate at the largest height fluctuation characterized by the amplitude h_S. For sinusoidal interfaces described by Eqs. (25) and (26) and using the noncrossing constraint (27), one obtains the inequality

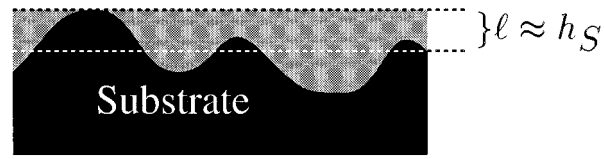

FIG. 4. Minimal mean film thickness l for which a flat liquid interface is still possible. The liquid interface touches the substrate surface at isolated points and the film thickness l corresponds to the characteristic corrugation amplitude h_S.

$$\overline{P^*}(l) > 0 \text{ for } h_S < l < \infty. \tag{31}$$

For smaller distances, the interaction $\overline{P^*}(l)$ can actually become negative with $\Delta\overline{\mathcal{F}^*}(l)$ still being strictly positive, because then the free energy expression (18) always has a positive-energy contribution from the interfacial tension of the liquid interface.

This result has consequences for the important class of wetting potentials with a single minimum at finite but rather large wetting film thickness, which describe continuous wetting transitions as the minimum moves outward to infinity. If the minimum occurs at distances larger than the roughness amplitude, it follows from Eq. (31) that the substrate roughness will not induce the wetting of the substrate.

From the above considerations we see that the interaction $\overline{P^*}(l)$ has to have rather complex behavior; at zero l or vanishing liquid film it is negative, since $\overline{P^*}(0) \approx \alpha_S S$, and we start with the assumption of a nonwetting behavior (i.e., $S < 0$) for the flat solid surface. Considering only the $l = 0$ situation, we see that there is a threshold value of the solid roughness in order to make the vanishing film limit energetically unfavorable compared to the infinite film limit; see Eq. (24). For a film thickness larger than the amplitude of the solid roughness, the interaction $\overline{P^*}(l)$ has to be repulsive in order to make roughness-induced wetting possible; see Eq. (31). The question that arises naturally is whether such a behavior is actually possible and what the conditions on the molecular interaction $w(\mathbf{r})$ are.

C. Sufficient condition for roughness-induced wetting

In this section, we want to show for general film thicknesses under which conditions roughness-induced wetting, as defined by Eq. (22), occurs. In order to do so, we need to minimize the free energy with respect to the fluid interface profile $\zeta_L(\boldsymbol{\rho})$ for each average film thickness l and for a

given molecular interaction $w(\boldsymbol{\rho},z)$ and interfacial tensions, according to Eq. (16) [with $\zeta_L(\boldsymbol{\rho})$ entering the expressions (8) and (9)]. We then have to check whether $\Delta\overline{\mathcal{F}}^*(l)>0$ holds for each l. If it turns out that $\Delta\overline{\mathcal{F}}^*(l)<0$ for a given l, we know that the system will prefer to have a stable film of this thickness and wetting will not occur.

For the present purpose, we turn this procedure somewhat around. We will try to determine the interaction for which roughness-induced wetting, for given values of the interfacial tensions and the substrate roughness, does occur. Furthermore, in many situations the molecular interaction $w(\boldsymbol{\rho},z)$ is not easily available, and usually the wetting potential for two flat interfaces $P^0(l)$, as defined by Eq. (2), is readily measured and calculated. We will therefore use a relation between the planar interaction $P^0(l)$ and the wetting potential between two sinusoidally modulated interfaces $P(\rho_1,l,h_L)$, which is derived in the Appendix. Using this relation, we express the condition for roughness-induced wetting in terms of a lower bound on the planar interaction $P^0(l)$. The analysis will be presented in the next two subsections. These parts are somewhat technical, and the unmotivated reader can easily skip these sections and move on to the results in Sec. III C 3.

1. Construction of lower bound on $P^0(l)$

To proceed, consider first the range $l<h_S$. In the tension-dominated regime, defined by $h_S q \ll 1$, it follows that $lq \ll 1$ also holds. In this limit, the wetting potential, defined by Eq. (9), can, for the special case of two sinusoidal interfaces (see Sec. III B 2), be expressed in terms of the planar interaction $P^0(l)$. Neglecting curvaturelike terms that turn out to scale like $h_S h_L q^4$, this relation is given by (see the Appendix)

$$P(\rho_1,l,h_L)\simeq(1+h_S h_L q^2\cos^2[q\rho_1])^{1/2} \times P^0\left(\frac{l+(h_S-h_L)\sin[q\rho_1]}{(1+h_S h_L q^2\cos^2[q\rho_1])^{1/2}}\right). \quad (32)$$

Clearly, the above form has the following desired property: for $l=0$ one has $h_L=h_S$ and one thus obtains for the spatially averaged potential $\overline{P}(l=0,h_L)\simeq\alpha_S P^0(l=0)$, as anticipated on intuitive grounds in the paragraph preceding Eq. 18. For either $h_S=0$ or $h_L=0$ the formula (32) simplifies to $P(\rho_1,l,h_L)=P^0(l+(h_S-h_L)\sin[q\rho_1])$, which is exact.

Still, the formula (32) is rather complicated and calculating the spatially averaged potential $\overline{P}(l,h_L)\equiv\langle P(\rho_1,l,h_L)\rangle_{\rho_1}$ is by no means trivial. The following observation is crucial. For a given value of l, the argument of P^0 in Eq. (32) is strictly smaller than $2l$ (since $2h_S l q^2<1$). We can therefore choose a linear trial function of the form

$$P_T^0(t)=S+c(l)t. \quad (33)$$

For a given value of l, we require the trial $P_T^0(t)$ to be a lower bound of the flat-interface potential $P^0(t)$, i.e., $P_T^0(t)<P^0(t)$, in the finite range $0\leqslant t\leqslant 2l$, which puts certain bounds on the slope $c(l)$. It trivially follows that $P(\rho_1,l,h_L)$ as given by Eq. (32) and evaluated with P_T^0 is always lower than $P(\rho_1,l,h_L)$ evaluated with P^0 instead.

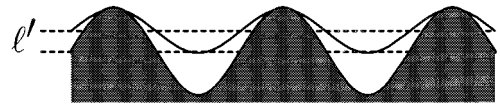

FIG. 5. Liquid film with a thickness l', for which the liquid interface with a corrugation amplitude h_L^* as given by Eq. (35) just touches the substrate. Since the two interfaces cannot cross, in the single q-mode approximation the amplitude h_L increases for smaller values of l until one finally obtains $h_L=h_S$ in the limit $l\to 0$. In a more realistic model, one might obtain a ruptured interface for small layer thicknesses, corresponding to separate droplets.

The strategy will be as follows. If we can show that for a film with a given average thickness l and using the linear trial function P_T^0 the resulting free energy difference $\Delta\overline{\mathcal{F}}^*(l)$ is positive, we know that the wetting film for this particular mean thickness is unstable. This follows since using P^0 instead of P_T^0 we will necessarily increase $\overline{P}^*(l)$ and thus also increase $\Delta\overline{\mathcal{F}}^*(l)$. If we succeed in showing the same for all values of l (including $l=0$), it follows that $P^0(l)$ (which is by construction strictly larger than all the linear trial functions) is an interaction that shows roughness-induced wetting. In the subsequent calculations we actually reverse this procedure and start with the linear trial functions, enforcing instability of the wetting film for each value of l separately [leading to restrictions on the l-dependent slopes $c(l)$], and construct the function $P^0(l)$ from a superposition of all piecewise linear functions. Choosing a linear trial function of the form (33), does not restrict the generality of our results, since one can express any function as the supremum of a set of suitable piecewise linear functions.

Using the trial function (33), the averaging over the coordinate ρ_1 can be easily done and, with Eqs. (18) and (32), the resultant trial free energy is given by

$$\Delta\overline{\mathcal{F}}_T(l,h_L)=\tfrac{1}{4}\gamma h_L^2 q^2+S(1+\tfrac{1}{4}h_S h_L q^2)+c(l)l+\mathcal{O}(q^4). \quad (34)$$

Minimizing this free-energy expression with respect to h_L, one obtains the amplitude

$$h_L^*=-\frac{S}{2\gamma}h_S, \quad (35)$$

which characterizes the minimizing liquid interface profile ζ_L^*. The liquid interface corrugation is in phase with the substrate configuration, since $S<0$. Since the two interfaces have to satisfy the noncrossing constraint (27), the minimizing amplitude h_L^* can be realized only for a thickness larger than some characteristic length $l\geqslant l'$. For $l=l'$, the liquid interface has an amplitude given by Eq. (35) and touches the substrate surface; this situation is depicted in Fig. 5. This defines the length l', which is, combining Eqs. (27) and (35), given by

$$l'=h_S\left(1+\frac{S}{2\gamma}\right). \quad (36)$$

For smaller film thicknesses l, the amplitude h_L necessarily deviates from the value h_L^* and finally equals h_S for $l=0$. Note that the length l' is always bounded by $h_S/2<l'<h_S$, as follows from the fact that $\gamma>-S$; see Eq. (23).

2. Calculation for $S_{\rm eff}=0$

In this section we assume that $S_{\rm eff}=0$, which means the substrate roughness just suffices to make the nonwetting state ($l=0$) energetically unfavorable compared to the completely wet state ($l=\infty$) at coexistence ($\mu=0$). This is obviously not necessary, but renders the resultant expressions in a simpler form and is sufficient for $\mu=0$. The extension to general $S_{\rm eff}$ will be done in Sec. III C 4. From Eq. (30) the excess substrate surface area $q^2h_S^2/4$ is given by

$$\frac{q^2h_S^2}{4}=-\frac{S}{S+\gamma}.$$

For $l<l'$, the amplitude that minimizes the free energy and is in accord with the noncrossing constraint is given by $h_L=h_S-l$, that is, the interfaces just touch. Inserting this amplitude into the trial free-energy expression (34), one obtains the minimal value (denoted by an asterisk)

$$\Delta\bar{\mathcal{F}}_T^*(l)=c(l)l-\frac{l^2}{h_S^2}\left(\frac{\gamma S}{S+\gamma}\right)+\frac{Sl}{h_S}\left(\frac{S+2\gamma}{S+\gamma}\right)\ \text{for}\ \ l<l'. \tag{37}$$

Thus the sufficient condition for the free-energy difference to be positive is

$$c(l)\geqslant-\frac{S}{h_S}\left(\frac{S+2\gamma}{S+\gamma}\right)+\frac{l}{h_S^2}\left(\frac{\gamma S}{S+\gamma}\right)\ \text{for}\ \ l<l', \tag{38}$$

with the special values

$$c(0)\geqslant-\frac{S}{h_S}\left(\frac{S+2\gamma}{S+\gamma}\right) \tag{39}$$

and

$$c(l')\geqslant-\frac{S}{2h_S}\left(\frac{S+2\gamma}{S+\gamma}\right). \tag{40}$$

For $l>l'$, one inserts the expression (35) found for h_L^* into the free energy (34) and obtains

$$\Delta\bar{\mathcal{F}}_T^*(l)=c(l)l+S-\frac{h_S^2S^2q^2}{16\gamma}\ \text{for}\ \ l>l'. \tag{41}$$

Using that $S_{\rm eff}=0$, it follows that

$$\Delta\bar{\mathcal{F}}_T^*(l)=c(l)l+S+\frac{S^3}{4\gamma(S+\gamma)}\ \text{for}\ \ l>l'. \tag{42}$$

In this case, requiring the free energy to be positive leads to the condition

$$c(l)\geqslant-\frac{S}{4\gamma l}\frac{(S+2\gamma)^2}{S+\gamma}\ \text{for}\ \ l>l'. \tag{43}$$

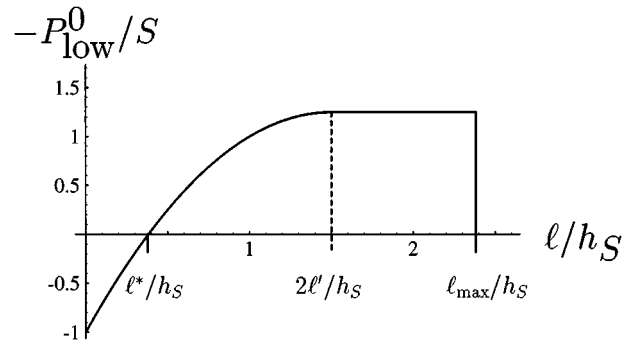

FIG. 6. Plot of the lower bound for wetting potentials $-P^0_{\rm low}/S$ as a function of the rescaled film thickness l/h_S, for $-S/\gamma=1/2$ and $S_{\rm eff}=0$. In the interval $0<l<2l'$, $P^0_{\rm low}(l)$ is a monotonically increasing function. In the interval $2l'<l<l_{\rm max}$, $P^0_{\rm low}(l)$ is constant. For $l>l_{\rm max}$ one finds $P^0_{\rm low}(l)=0$. The value l^* is defined by $P^0_{\rm low}(l^*)=0$.

with the limiting value (40) for $l=l'$.

Thus far, we have calculated a lower bound of the planar potential $P^0(t)$ for a given value of the average film thickness l, which consists of a linear function of finite extent (between 0 and $2l$) and l-dependent slope. In order to construct a lower bound on $P^0(t)$ that is valid for *any* film thickness, we have to calculate the upper envelope of these linear functions. This function we denote by $P^0_{\rm low}(l)$. The sufficient condition for wetting, corresponding to the definition (22), can then be written as

$$P^0(l)>P^0_{\rm low}(l), \tag{44}$$

with $P^0_{\rm low}(l)$ being defined as

$$P^0_{\rm low}(l)\equiv\max_{t\geqslant l/2}\{S+c(t)l\}. \tag{45}$$

The value of $c(t)$ is given by Eqs. (38) and (43) for $t<l'$ and $t>l'$, respectively. Since $c(t_1)>c(t_2)$ holds for any $t_1<t_2$, it is easy to see that the function $P^0_{\rm low}(l)$ can be expressed in closed form as

$$P^0_{\rm low}(l)=S+c(l/2)l. \tag{46}$$

Using the expressions (38) and (43), the function $P^0_{\rm low}(l)$ is explicitly given by

$$P^0_{\rm low}(l)=\begin{cases} S\left(1-\dfrac{l}{h_S}\dfrac{S+2\gamma}{S+\gamma}+\dfrac{l^2}{h_S^2}\dfrac{\gamma/2}{S+\gamma}\right) & \text{for}\quad l\leqslant 2l' \\ S\left(1-\dfrac{(S+2\gamma)^2}{2\gamma(S+\gamma)}\right) & \text{for}\quad 2l'\leqslant l\leqslant l_{\rm max} \\ 0 & \text{for}\quad l>l_{\rm max}. \end{cases} \tag{47}$$

3. Results for $S_{\rm eff}=0$

Figure 6 shows the rescaled lower bound $-P^0_{\rm low}/S$ as a function of the rescaled variable l/h_S for $-S/\gamma=1/2$. This function starts out at -1 for $l/h_S=0$ by definition of the

spreading coefficient S. The slope at the origin is finite and the function increases until it reaches its maximum at $l=2l'$. We obtain a plateau in the interval $2l'<l<l_{\max}$; for $l>l_{\max}$ the lower bound is given by $-P^0_{\rm low}(l)/S=0$. In our estimate for the value of $l_{\max}$ we set $l_{\max}=l^*+2h_S$, where l^* is defined by $P^0_{\rm low}(l^*)=0$ (see Fig. 6). This is based on the observation that for $l>l_{\max}$ the interaction as given by Eq. (32) is strictly positive as long as $|h_L|<h_S$, since in this case the arguments of P^0 in Eq. (32) are always larger than l^*; consequently, the free-energy difference (18) will be always positive. If, on the other hand, $|h_L|>h_S$ holds, the free energy difference (18) will also be positive since then $\alpha_L(l,h_L)>\alpha_L(0)$ and $\overline{P^*}(l)>\overline{P^*}(0)$ holds for any $l>0$.

The value for l^* as obtained from Eq. (47) is given by

$$\frac{l^*}{h_S}=\frac{S+2\gamma}{\gamma}-\sqrt{\left(\frac{S+2\gamma}{\gamma}\right)^2-\frac{2(S+\gamma)}{\gamma}} \tag{48}$$

and reduces to the value $l^*/h_S\approx 2-\sqrt{2}\approx 0.59$ in the tension-dominated regime $\gamma\gg -S$ and approaches zero in the interaction dominated regime $\gamma\gtrsim -S$. The largest possible value for $l_{\max}/h_S$ is thus $l_{\max}/h_S=4-\sqrt{2}\approx 2.59$. In the tension-dominated regime $\gamma\gg -S$, the assumption we started with $lq\ll 1$ thus holds for the whole range of thicknesses considered because the substrate roughness necessary to achieve roughness-induced wetting is small $h_S q\ll 1$. In the same limit, the general expression (47) takes the values

$$P^0_{\rm low}(l)\approx\begin{cases} S\left(1-2\dfrac{l}{h_S}+\dfrac{1}{2}\dfrac{l^2}{h_S^2}\right) & \text{for} \quad l/h_S\leqslant 2 \\ -S & \text{for} \quad 2\leqslant l/h_S\leqslant 4-\sqrt{2} \\ 0 & \text{for} \quad l/h_S>4-\sqrt{2}. \end{cases} \tag{49}$$

In the interaction dominated regime, for $\gamma\gtrsim -S$, the maximum of $P^0_{\rm low}(l)$ for $2l'\leqslant l\leqslant l_{\max}$ actually diverges as $\gamma\to -S$, with $2l'/h_S\to 1$ and $l_{\max}/h_S\to 2$. Note that in this regime, also the substrate roughness necessary to induce wetting goes to infinity; see Eq. (24). It follows that it is the tension-dominated regime where roughness-induced is most likely to be observed experimentally.

The function $P^0_{\rm low}(l)$ as given by Eq. (47) is plotted in Fig. 7 for $-S/\gamma=0$, 1/2, and 2/3, from bottom to top. As this ratio becomes larger, as one moves from the tension-dominated regime into the interaction-dominated regime, the maximum of $-P^0_{\rm low}(l)/S$ increases, until it finally reaches infinity for $-\gamma/S=1$.

The interpretation of the results in Fig. 7 is the following. For a given ratio of the spreading coefficient S and the liquid interfacial tension γ, which are determined by the interfacial tensions of the problem alone and conspire to give $S_{\rm eff}=0$, one rescales the amplitude of the wetting potential $P^0(l)$ (which can be measured or calculated theoretically) by the spreading coefficient and the distance l by the roughness amplitude h_S. If the rescaled potential $-P^0(l/h_S)/S$ is

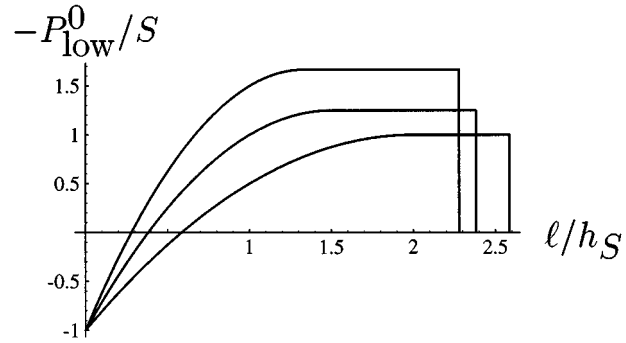

FIG. 7. Plot of the lower bound for wetting potentials $-P^0_{\rm low}/S$ as a function of the rescaled film thickness l/h_S, in the limit $\gamma\gg -S$, for $-S/\gamma=1/2$ and for $-S/\gamma=2/3$ (from bottom to top). The curves shown correspond to the special case $S_{\rm eff}=0$, i.e., the relative area of the substrate is just sufficient to make the free energy of the dry state ($l=0$) higher than the completely wet state ($l=\infty$). The area ratios are given by $\alpha_S=1$, 2, and 3, from bottom to top.

larger than $-P^0_{\rm low}(l/h_S)/S$ for all arguments, i.e., if the sufficient condition (44) is fulfilled, a complete wetting situation will result.

An interesting feature of our results comes from the fact that we obtain universal lower bounds as a function of the film thickness l rescaled by the roughness amplitude h_S. This suggests that there exists for a given substrate excess surface area $\sim h_S^2q^2/4$ an optimal value of the roughness amplitude h_S for roughness-induced wetting to occur. Since the maximum of the lower bound $-P^0_{\rm low}(l/h_S)/S$ is located at $l/h_S\approx 1$, this optimal value of h_S happens to coincide with the approximate location of the maximum of $P^0(l)$, the wetting potential. Assume that the sufficient condition (45) is in fact satisfied for this optimal value of h_S. For roughness amplitudes much smaller than this optimal value (the function P^0 will be pushed to the right in the scaling plot Fig. 7) the sufficient condition cannot be satisfied for very small film thicknesses due to the finite slope of the wetting potential, suggesting an infinitesimally thin stable film (no wetting). For roughness amplitudes much larger than the optimal value (the function P^0 will be squeezed to the left in Fig. 7) the sufficient condition is not satisfied for average film thicknesses larger than some value at the order of the roughness amplitude, suggesting the formation of a very thin liquid film occupying preferentially the valleys of the substrate surface fluctuations (partial prewetting).

4. Results for general $S_{\rm eff}$

Here we treat the general case with $S_{\rm eff}>0$, now including the cases where the substrate roughness α_S is larger than the necessary value obtained by setting $S_{\rm eff}=0$ in Eq. (21). In addition, we will require the free-energy difference (18) to be larger than a constant denoted by $\mathcal{F}_0$, as will turn out to be important if one looks at stable wetting layers in the presence of a chemical potential (see Sec. III D). Using a trial function of the form (33), the following bounds for the slope $c(l)$ follow

$$c(l) \geqslant \frac{1}{h_S} \begin{cases} \dfrac{(S+2\gamma)(S_{\rm eff}-S)}{S+\gamma} - \dfrac{l}{h_S^2}\dfrac{\gamma(S_{\rm eff}-S)}{S+\gamma} + \dfrac{\mathcal{F}_0 - S_{\rm eff}}{l} & \text{for } l<l' \\ \dfrac{\mathcal{F}_0}{l} + \dfrac{S^2 S_{\rm eff} - S(S+2\gamma)^2}{4\gamma l(S+\gamma)} & \text{for } l>l'. \end{cases} \tag{50}$$

(51)

Since $c(l)$ for $l<l'$ now is nonmonotonic and has a maximum at $\bar{l}$ given by

$$\bar{l} = h_S \sqrt{\frac{(S+\gamma)(S_{\rm eff}-\mathcal{F}_0)}{\gamma(S_{\rm eff}-S)}}, \tag{52}$$

the global lower bound $P^0_{\rm low}(l)$ can be calculated according to Eq. (46) only in the restricted range of $2\bar{l}<l<2l'$. For $l<2\bar{l}$, the function $P^0_{\rm low}(l)$ as defined by Eq. (45) has a constant slope of $c(l)$ given by Eq. (50) since $\bar{l}<l'$ strictly holds. The global lower bound is thus given by

$$P^0_{\rm low}(l) = \begin{cases} S + \dfrac{l}{h_S(S+\gamma)}\left[(S_{\rm eff}-S)(S+2\gamma) - 2\sqrt{\gamma(S_{\rm eff}-\mathcal{F}_0)(S_{\rm eff}-S)(S+\gamma)}\right] & \text{for } l \leqslant 2\bar{l} \\ S + 2(\mathcal{F}_0 - S_{\rm eff}) + \dfrac{l}{h_S}\dfrac{(S+2\gamma)(S_{\rm eff}-S)}{S+\gamma} - \dfrac{l^2}{h_S^2}\dfrac{\gamma(S_{\rm eff}-S)}{2(S+\gamma)} & \text{for } 2\bar{l} \leqslant l \leqslant 2l' \\ S + 2\mathcal{F}_0 + \dfrac{S_{\rm eff}S^2 - S(S+2\gamma)^2}{2\gamma(S+\gamma)} & \text{for } 2l' \leqslant l \leqslant l_{\max} \\ \mathcal{F}_0 & \text{for } l > l_{\max} \end{cases} \tag{53}$$

In Fig. 8 we plot $P^0_{\rm low}(l)$ for the fixed value $-S/\gamma = 1/2$ and the values $S_{\rm eff}=0$, $S_{\rm eff}/S=-1$, and $S_{\rm eff}/S=-2$ (from bottom to top in the right portion in the graphs). The interesting feature is that the plateau of $P^0_{\rm low}(l)$ for $l>2l'$ increases with increasing $S_{\rm eff}$. This indicates that for a given wetting potential $P^0(l)$ and a given roughness amplitude h_S the roughness-induced wetting transition might disappear for wave numbers much larger than the threshold value determined by Eq. (30).

D. Stable films in the presence of a chemical potential

So far, we have calculated a lower bound for the interaction, denoted by $P^0_{\rm low}(l)$, so that the free-energy difference $\Delta\bar{\mathcal{F}}^*(l)$ is positive [Eq. (37)] or larger than a positive constant $\mathcal{F}_0$ [Eq. (43)] for all values of l. If $P^0(l) \geqslant P^0_{\rm low}(l)$ holds and the chemical potential vanishes, i.e., at coexistence, the substrate will be covered with an infinitely thick liquid layer. For nonzero chemical potential, however, the substrate will always be covered with a film of *finite* thickness. For the sake of clarity, let us assume the potential $P^0(l)$ to have a single maximum at finite separation, decay for large separations like $P^0(l) \sim a l^{-\sigma}$ [where $\sigma = m-4$ if the molecular interaction is given by Eq. (A7)], and be negative for zero separation, corresponding to the nonwetting situation for a flat substrate. One notes that $\sigma=2$ for nonretarded van der Waals interactions.

For finite chemical potential, the free energy then has a minimum at a finite separation $l_{\min}$. Assuming that $l_{\min} \gg q^{-1}$, one can use Eq. (A21) and finds the leading terms of the free energy according to Eq. (18),

$$\Delta\bar{\mathcal{F}}(l,h_L) = \frac{\gamma}{4}h_L^2 q^2 + P^0(l) + \frac{1}{4}(h_S^2 + h_L^2)P^{\rm II}(l) + \mu l, \tag{54}$$

where the chemical potential term has been added. For a potential of the asymptotic form $\sim a l^{-\sigma}$ this free energy is minimized by $h_L=0$ and the film thickness that is stable with respect to variations in l is asymptotically given by

$$l_{\min} \sim (a\sigma/\mu)^{1/(1+\sigma)}. \tag{55}$$

Choosing the constant $\mathcal{F}_0$ in Eq. (53) to be $\mathcal{F}_0 = \Delta\bar{\mathcal{F}}^*(l_{\min}) = \Delta\bar{\mathcal{F}}(l_{\min}, h_L=0)$ and demanding $P^0(l)$

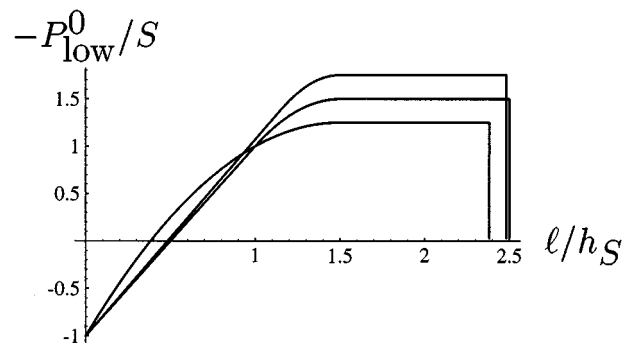

FIG. 8. Plot of the lower bound for wetting potentials $-P^0_{\rm low}/S$ as a function of the rescaled film thickness l/h_S, for the fixed value $-S/\gamma=1/2$ and for $S_{\rm eff}=0$, $-S$, and $=-2S$ (from bottom to top for the right portion of the plots). The relative area increase of the rough substrate is given by $\alpha_S=2$, 3, and 4, from bottom to top.

$>P^0_{\rm low}(l)$ as given by Eq. (53), the minimum at $l_{\rm min}$ is indeed the global minimum and we have a stable wetting film of finite thickness. We will now do a local stability analysis for this free-energy minimum. The linearized Euler equation, determining the stable liquid interface profile, can be obtained from the free energy expression (8) by requiring local force equilibrium $\partial\mathcal{F}(\boldsymbol{\rho},[\zeta_L])/\partial\zeta_L(\boldsymbol{\rho})=0$ and is given by

$$\gamma\triangle\zeta_L(\boldsymbol{\rho})+\Pi^0(l)-\int d^2\boldsymbol{\rho}'\{\zeta_L(\boldsymbol{\rho})-\zeta_S(\boldsymbol{\rho}+\boldsymbol{\rho}')-l\}w(\boldsymbol{\rho}',l)=\mu, \tag{56}$$

where $\Pi^0(l)\equiv -dP^0(l)/dl$ is the disjoining pressure for flat interfaces. Assuming the wetting layer to have a thickness corresponding to the global minimum as given by Eq. (55), which is equivalent to setting $\Pi^0(l_{\rm min})=\mu$ and approximating the interfacial profiles again by sinusoidal waves [Eqs. (25) and (26)], the locally stable liquid interface amplitude turns out to be [5]

$$h_L=\frac{h_S\int d^2\boldsymbol{\rho}\ \cos(q\rho_1)w(\boldsymbol{\rho},l)}{\gamma q^2+\int d^2\boldsymbol{\rho}\ w(\boldsymbol{\rho},l)}. \tag{57}$$

Using formulas (A9) and (A25), this amplitude scales like $h_L\sim h_S\exp(-ql)l^{1/2-m/2}q^{m/2-7/2}$ in the limit $ql\gg 1$; for van der Waals forces $(m=6)$ one obtains $h_L\sim h_S\exp(-ql)l^{-5/2}q^{-1/2}$. In contrast to the global stability analysis leading to Eq. (55), where we averaged over the spatial coordinate $\boldsymbol{\rho}$, the local equilibrium analysis now actually gives a nonvanishing amplitude h_L. Inserting this amplitude back into the free-energy expression (54), the stable film thickness is increased. However, the correction turns out to be less singular for the case of van der Waals forces and thus does not affect the asymptotic behavior of $l_{\rm min}$ as given by Eq. (55).

IV. DISCUSSION

Some necessary conditions for roughness-induced wetting have been obtained on very general grounds. First, the tension of the liquid interface has to be larger than the negative spreading coefficient or, equivalently, the tension of the substrate-vapor interface has to be larger than the tension of the substrate-liquid interface. Second, the roughness of the substrate, measured by the excess area as compared to the flat substrate, has to exceed a certain threshold; see Eq. (24). Using an approach that is equivalent to a linear-response analysis, we obtain a formula relating the molecular interaction between two rough interfaces to the interaction of two flat interfaces; the latter is the so-called wetting potential. Using this formula, a lower bound for wetting potentials in order to obtain this type of wetting transition is derived. This lower bound constitutes a sufficient condition. More specifically, this lower bound has the following properties: (i) for vanishing liquid film, or for zero separation between the two interfaces bounding the liquid layer, the interaction (which for this limit is the so-called spreading coefficient) is negative, corresponding to a nonwetting situation in the case of flat interfaces; (ii) the lower bound has a pronounced maximum with a height of at least the negative spreading coefficient at a separation of about the roughness amplitude. This height depends on the ratio between the liquid-interface tension γ and the spreading coefficient S.

These results concerning the possibility of a roughness-induced wetting transition agree with the very recent experimental observation of premelting induced by substrate roughness at the glass-ice interface [25], where glass surfaces showing a roughness with typical amplitudes of ~ 1 nm induced a complete interfacial premelting. Independently, the calculation of the dispersion interaction between half spaces of glass and ice separated by a liquid water layer show a pronounced maximum at about the same distance ~ 1 nm [35], consistent with our prediction for the lower bound of the wetting potential. We find the asymptotic behavior of the film thickness as a function of the chemical potential to be characterized by the standard van der Waals exponent, as shown in Sec. III D. This is in disagreement with the experimentally measured exponent $\simeq 2$ [25], which is to be contrasted with the exponent 1/3 as expected for nonretarded van der Waals interactions in the absence of any other interactions. Finally, we note that the interfacial energies for the case of interfacial premelting are influenced by grain-boundary energies in the disordered polycrystalline layers adjacent to the microscopically irregular substrate wall. In fact, it was argued [36] that this effect could independently lead to a roughness-induced premelting transition. Such a mechanism could be described within our framework by assuming an interfacial energy γ that depends explicitly on the roughness magnitude of the liquid interface. A further interesting effect might appear for the case of surface triple-point premelting: Here a roughness-induced complete surface melting could be triggered by a roughening transition of the solid surface [37]. Another interesting consequence of our results is that a discontinuous wetting transition might be converted into a continuous transition by a change of the effective wetting potential at small distances.

Our calculations are most valid for small substrate roughness, as defined by $h_S q<1$; this also seems to be the experimentally most relevant limit, since rough surfaces produced by etching usually show modest corrugation amplitudes [34]. The closed-form expressions for the interaction of two corrugated interfaces obtained in the Appendix are, to the best of our knowledge, novel and applicable to a wide range of phenomena, including dewetting phenomena (where the whole argument has to be inverted, leading to roughness-induced dewetting). We also derive an expression for the curvature contribution to the free energy, which might play a role in the adsorption of membranes or vesicles on rough substrates.

ACKNOWLEDGMENTS

This project initiated when one of us (D.A.) visited the laboratory of D. Beaglehole. He is grateful to D. Beaglehole for introducing him to the subject of roughness-induced wetting, for sharing with him his experimental results prior to publication, and for his hospitality. D.A. acknowledges partial support from the German Israel Foundation under Grant No. I-0197 and the U.S.—Israel Binational Science Foundation under Grant No. 94-00291. R.N. acknowledges support from the Minerva Foundation, receipt of a NATO stipend administered by the DAAD, and partial support by the Na-

tional Science Foundation under Grant No. DMR-9220733. We would like to thank G. Dash, S. Dietrich, M. Elbaum, F. Joanny, S. Safran, M. Schick, U. Steiner, J. Wettlaufer, and L. Wilen for helpful discussions.

APPENDIX: DERIVATION OF THE EFFECTIVE POTENTIAL

The total interaction per unit (projected) area between the liquid interface at lateral position $\boldsymbol{\rho}$ located at $\zeta_L(\boldsymbol{\rho})$ and a corrugated solid surface, parametrized by $\zeta_S(\boldsymbol{\rho})$ (see Fig. 3), can be written as

$$P(\boldsymbol{\rho},[\zeta_L])=\int_{\zeta_L(\boldsymbol{\rho})}^{\infty}dz\int d^2\boldsymbol{\rho}'\int_{-\infty}^{\zeta_S(\boldsymbol{\rho}+\boldsymbol{\rho}')}dz'\,w(\boldsymbol{\rho}',z-z'). \tag{A1}$$

This expression is hard to deal with due to the nonlocal dependence on the shape of the solid surface, which enters in the integration boundary. Progress can be made by formally expanding $\zeta_S(\boldsymbol{\rho}+\boldsymbol{\rho}')$ around $\zeta_L(\boldsymbol{\rho})-l$. The average separation between the two interfaces l is given by $l\equiv\langle\zeta_L(\boldsymbol{\rho})-\zeta_S(\boldsymbol{\rho})\rangle$, where the angular brackets denote a spatial average over $\boldsymbol{\rho}$.

Keeping terms up to fourth order, one obtains

$$\begin{aligned}P(\boldsymbol{\rho},[\zeta_L])=&P^0(l)+\int_l^{\infty}dz\int d^2\boldsymbol{\rho}'[\zeta_S(\boldsymbol{\rho}+\boldsymbol{\rho}')\\&-\zeta_L(\boldsymbol{\rho})+l]w(\boldsymbol{\rho}',z)+\frac{1}{2}\int d^2\boldsymbol{\rho}'[\zeta_S(\boldsymbol{\rho}+\boldsymbol{\rho}')\\&-\zeta_L(\boldsymbol{\rho})+l]^2w(\boldsymbol{\rho}',l)+\frac{1}{6}\int d^2\boldsymbol{\rho}'[\zeta_S(\boldsymbol{\rho}+\boldsymbol{\rho}')\\&-\zeta_L(\boldsymbol{\rho})+l]^3\frac{\partial}{\partial z}w(\boldsymbol{\rho}',z)|_{z=l}\\&+\frac{1}{24}\int d^2\boldsymbol{\rho}'[\zeta_S(\boldsymbol{\rho}+\boldsymbol{\rho}')-\zeta_L(\boldsymbol{\rho})+l]^4\\&\times\frac{\partial^2}{\partial z^2}w(\boldsymbol{\rho}',z)|_{z=l},\end{aligned} \tag{A2}$$

where the expression for the interaction of two planar surfaces introduced in Eq. (2),

$$P^0(l)\equiv\int_l^{\infty}dz\int d^2\boldsymbol{\rho}\int_{-\infty}^{0}dz'\,w(\boldsymbol{\rho},z-z'), \tag{A3}$$

has been used. At this point it is useful to specify the interfacial profiles; we choose one-dimensional sinusoidal profiles for the liquid and the solid surfaces, as depicted in Fig. 3, as is sufficient and appropriate for a linear analysis,

$$\zeta_S(\boldsymbol{\rho})\equiv\zeta_S(\rho_1)=h_S\sin[q(\rho_1)], \tag{A4}$$

$$\zeta_L(\boldsymbol{\rho})\equiv\zeta_L(\rho_1)=h_L\sin[q\rho_1]+l. \tag{A5}$$

Now the expression (A2) can be averaged over the $\boldsymbol{\rho}$-coordinates, thus yielding the mean interaction $P(l,[\zeta_L])\equiv\langle P(\boldsymbol{\rho},[\zeta_L])\rangle_{\boldsymbol{\rho}}$, which for sinusoidal interfacial profiles reads

$$\begin{aligned}\overline{P(l,h_L)}=&P^0(l)+\frac{1}{4}\int d^2\boldsymbol{\rho}(h_S^2+h_L^2-2h_Sh_L\cos[q\rho_1])w(\boldsymbol{\rho},l)\\&+\frac{1}{64}\int d^2\boldsymbol{\rho}\{h_S^4+h_L^4+4h_S^2h_L^2\\&-4h_Sh_L(h_S^2+h_L^2)\cos[q\rho_1]\\&+2h_S^2h_L^2\cos[2q\rho_1]\}\frac{\partial^2}{\partial z^2}w(\boldsymbol{\rho},z)|_{z=l}\end{aligned} \tag{A6}$$

and is an expansion up to fourth order in the interface modulation amplitudes h_S and h_L.

To proceed further, it is appropriate to specify the molecular interaction $w(\boldsymbol{\rho},z)$. In all that follows, an inverse power law defined by

$$w(\boldsymbol{\rho},z)\equiv A(\rho^2+z^2)^{-m/2} \tag{A7}$$

will be used. Accordingly, nonretarded van der Waals interactions correspond to $m=6$ with A being the Hamaker constant. The interaction between planar surfaces is given by

$$P^0(l)=\frac{2\pi A}{(m-2)(m-3)(m-4)}l^{4-m}. \tag{A8}$$

In addition, the following relations involving derivatives of $P^0(l)$ turn out to be useful:

$$P^{(\mathrm{II})}(l)=\frac{2\pi A}{m-2}l^{2-m}=A\int d^2\boldsymbol{\rho}(\rho^2+l^2)^{-m/2}, \tag{A9}$$

$$P^{(\mathrm{IV})}(l)=2\pi A(m-1)l^{-m}, \tag{A10}$$

$$P^{(-\mathrm{II})}(l)=\frac{2\pi A}{(m-2)(m-3)(m-4)(m-5)(m-6)}l^{6-m}, \tag{A11}$$

where $d^2P^{(\mathrm{-II})}(l)/dl^2=P^0(l)$. Note that $P^{(-II)}(l)$ is not defined for van der Waals interactions with $m=6$; this important case will be considered separately.

The terms in Eq. (A6) involving a cosine can now be evaluated analytically; for the first term, and using the interaction defined in Eq. (A7), we obtain

$$\begin{aligned}&A\int_{-\infty}^{\infty}d\rho_1\int_{-\infty}^{\infty}d\rho_2\frac{\cos[q\rho_1]}{(\rho_1^2+\rho_2^2+l^2)^{m/2}}\\&=\frac{A\sqrt{\pi}\Gamma\left(\frac{m-1}{2}\right)}{\Gamma\left(\frac{m}{2}\right)}\int_{-\infty}^{\infty}d\rho_1\frac{\cos[q\rho_1]}{(\rho_1^2+l^2)^{(m-1)/2}}.\\&=\frac{2\pi A}{\Gamma\left(\frac{m}{2}\right)}K_{m/2-1}(ql)(ql)^{m/2-1}l^{2-m}2^{1-m/2}.\end{aligned} \tag{A12}$$

In Eq. (A12) $K_\nu(z)$ denotes the modified Bessel function in standard notation.

1. Small separations

Let us first concentrate on separations l much smaller than the typical wavelength q^{-1} of the surface corrugation, i.e., $l \ll q^{-1}$. For small values of the argument z, the product $K_\nu(z)z^\nu$ can be expanded as a power series

$$K_\nu(z)z^\nu = a_0 + a_2 z^2 + a_4 z^4 + \cdots, \tag{A13}$$

with $\nu = m/2 - 1$ and the coefficients given by

$$a_0 = 2^{\nu-1}\Gamma(\nu) \quad \text{for} \quad \nu > 0, \tag{A14}$$

$$a_2 = -2^{\nu-3}\Gamma(\nu-1) \quad \text{for} \quad \nu > 1, \tag{A15}$$

$$a_4 = 2^{\nu-6}\Gamma(\nu-2) \quad \text{for} \quad \nu > 2. \tag{A16}$$

Note that for van der Waals forces, characterized by $\nu = 2$, the coefficient a_4 is given by

$$a_4 = (3/2 - 2\gamma + 2\ln 2 - 2\ln z)/16. \tag{A17}$$

with γ being the Euler constant defined by $\gamma = 0.577\,21$. Using this expansion and the definitions (A8)–(A11), the cosine term in Eq. (A6) can be written as

$$\begin{aligned} A\int_{-\infty}^{\infty} d\rho_1 \int_{-\infty}^{\infty} d\rho_2 \frac{\cos[q\rho_1]}{(\rho_1^2+\rho_2^2+l^2)^{m/2}} &= P^{(\mathrm{II})}(l) - \frac{m-3}{2} q^2 P^0(l) + \frac{(m-3)(m-5)}{8} \\ &\quad \times q^4 P^{(-\mathrm{II})}(l) + O(q^6). \end{aligned} \tag{A18}$$

For the case of van der Waals interactions $m = 6$, one analogously obtains

$$\begin{aligned} A\int_{-\infty}^{\infty} d\rho_1 \int_{-\infty}^{\infty} d\rho_2 \frac{\cos[q\rho_1]}{(\rho_1^2+\rho_2^2+l^2)^{3}} &= \frac{2\pi}{4}\left(\frac{1}{l^4} - \frac{q^2}{4l^2} + \frac{3-4\gamma+4\ln 2-4\ln(ql)}{64} q^4\right) \\ &\quad + O(q^6), \end{aligned} \tag{A19}$$

which includes a logarithmic singularity for small separations.

For the other term in Eq. (A6) involving a cosine one can interchange the differentiation and integration (for $m > 6$); the additional integral needed involves $\cos[2q\rho_1]$ and is given by

$$\begin{aligned} A\int_{-\infty}^{\infty} d\rho_1 \int_{-\infty}^{\infty} d\rho_2 \frac{\cos[2q\rho_1]}{(\rho_1^2+\rho_2^2+l^2)^{m/2}} &= P^{(\mathrm{II})}(l) - 2(m-3)q^2 P^0(l) \\ &\quad + 2(m-3)(m-5)q^4 P^{(\text{-II})}(l). \end{aligned} \tag{A20}$$

Using the formulas (A18) and (A20), and the definitions (A8c) and (A11), one obtains the following expansion for Eq. (A6):

$$\begin{aligned} \overline{P}(l,h_L) &= P^0(l)\left[1 + \frac{m-3}{4} h_S h_L q^2 - \frac{(m-3)(m-5)}{128} h_S h_L (h_S - h_L)^2 q^4 + \frac{3(m-3)(m-5)}{64} h_S^2 h_L^2 q^4\right] \\ &\quad + P^{(\mathrm{II})}(l)\left[\frac{1}{4}(h_S-h_L)^2 + \frac{m-3}{32} h_S h_L (h_S-h_L)^2 q^2\right] \\ &\quad + P^{(\mathrm{IV})}(l)\frac{1}{64}(h_S-h_L)^4 - \delta\overline{P}(l,h_L) \\ &\quad + O(h^6, q^6), \end{aligned} \tag{A21}$$

which is valid for $ql \ll 1$ and $m > 4$ (for $m = 4$ additional logarithmic singularities appear in terms proportional to q^2). The terms up to $O(h^2, q^2)$ have been obtained previously in the context of the dynamics of thin wetting layers [38]. The correction term $\delta\overline{P}$ corresponds to a curvature contribution and is given up to $O(h^4, q^4)$ by

$$\delta\overline{P}(l,h_L) = \frac{(m-3)(m-5)}{16} P^{(-\mathrm{II})}(l) h_S h_L q^4. \tag{A22}$$

This curvature contribution has additional nonanalytic terms for the case of nonretarded van der Waals interactions $m = 6$; for this case, one obtains

$$\delta\overline{P}(l,h_L) = \frac{\pi}{256}\,\frac{3-4\gamma+4\ln 2-4\ln(ql)}{64} h_S h_L q^4. \tag{A23}$$

The same singularity $\sim q^4 \ln q$ has been found for a free interface in the presence of van der Waals forces [26].

2. Large separations

In the other limit, for $ql \gg 1$, the product $K_\nu(z)z^\nu$ is given by

$$K_\nu(z)z^\nu = \sqrt{\pi/2}\, z^{\nu-1/2} e^{-z}[1 + (4\nu^2-1)/8z + \cdots]. \tag{A24}$$

In this case, the expression (A12) is asymptotically given by

$$A\int_{-\infty}^{\infty} d\rho_1 \int_{-\infty}^{\infty} d\rho_2 \frac{\cos[q\rho_1]}{(\rho_1^2+\rho_2^2+l^2)^{m/2}} = \frac{2^{3/2-m/2}\pi^{3/2} A}{\Gamma\left(\frac{m}{2}\right)} q^{m/2-3/2} l^{1/2-m/2} e^{-ql} \tag{A25}$$

From Eq. (A6) one immediately obtains

$$\overline{P(l,h_L)} = P^0(l) + \frac{1}{4}P^{(\mathrm{II})}(l)(h_S^2+h_L^2) + \frac{1}{64}P^{(\mathrm{IV})}(l)(h_S^4+h_L^4+4h_S^2h_L^2) + O(e^{-ql}), \tag{A26}$$

which is valid for $ql \gg 1$.

3. Closed-form expressions for the effective potential

In the following, formulas are presented, which express the series for the effective interaction between the two rough interfaces (A21) and (A26) in terms of the interaction $P^0(l)$ between two flat interfaces. For the case $ql \ll 1$, this expression is given by

$$P(\rho_1,l,h_L) = (1+h_Sh_Lq^2\cos^2[q\rho_1])^{1/2}P^0 \times \left(\frac{l+(h_S-h_L)\sin[q\rho_1]}{(1+h_Sh_Lq^2\cos^2[q\rho_1])^{1/2}}\right) - \delta P(\rho_1,l,h_L). \tag{A27}$$

For the case $ql \gg 1$, the corresponding expression is given by

$$P(\rho_1,l,h_L) = \langle P^0(l+h_L\sin[q\rho_1]+h_S\sin[q\tau_1])\rangle_{\tau_1} + O(e^{-ql}), \tag{A28}$$

where τ_1 is the local lateral coordinate on the liquid interface and is averaged over, leaving only the dependence on the coordinate ρ_1 in the substrate interface. Expressions (A27) and (A28) depend explicitly on the spatial coordinate ρ_1; that they indeed reproduce term by term the series (A21) and (A26) can be checked by expansion and averaging over ρ_1. The validity of the closed-form expression is thus proven for power laws with arbitrary m; we were not able to extend this proof to interactions that include a cutoff at small separations. However, it is likely that the formulas (A27) and (A28) are also accurate for potentials $P^0(l)$ that do not diverge as $l \to 0$. This is supported by the fact that for $l=0$ the formula (A27) exactly describes the surfacelike energy contributions.

[1] P.-G. de Gennes, Rev. Mod. Phys. **57**, 827 (1985).
[2] S. Dietrich, in *Phase Transitions and Critical Phenomena*, edited by C. Domb and J. Lebowitz (Academic, New York, 1988), Vol. 12.
[3] M. Schick, in *Liquids at Interfaces*, Proceedings of the Les Houches Summer School of Theoretical Physics Session XLVIII, edited by J. Charvolin, J.-F. Joanny, and J. Zinn-Justin (Elsevier, Amsterdam, 1990).
[4] J.G. Dash, Contemp. Phys. **30**, 89 (1989).
[5] D. Andelman, J.-F. Joanny, and M.O. Robbins, Europhys. Lett. **7**, 731 (1988); M.O. Robbins, D. Andelman, and J.-F. Joanny, Phys. Rev. A **43**, 4344 (1991); J.L. Harden and D. Andelman, Langmuir **8**, 2547 (1992).
[6] P. Pfeiffer, Y.J. Wu, M.W. Cole, and J. Krim, Phys. Rev. Lett. **62**, 1997 (1989).
[7] M. Kardar and J.O. Indekeu, Europhys. Lett. **12**, 161 (1990).
[8] M. Napiórkowski, W. Koch, and S. Dietrich, Phys. Rev. A **45**, 5760 (1992).
[9] A. Korociínski and M. Napiórkowski, Mol. Phys. **84**, 171 (1995).
[10] D. Beaglehole, J. Phys. Chem. **93**, 893 (1989).
[11] S. Garoff, E.B. Sirota, S.K. Sinha, and H.B. Stanley, J. Chem. Phys. **90**, 7505 (1989).
[12] I.M. Tidswell, T.A. Rabedeau, P.S. Pershan, and S.D. Kosowsky, Phys. Rev. Lett. **66**, 2108 (1991); P.S. Pershan, Ber. Bunsenges. Phys. Chem. **98**, 372 (1994).
[13] P. Müller-Buschbaum, M. Tolan, W. Press, F. Brinkop, and J.P. Kotthaus, Ber. Bunsenges. Phys. Chem. **98**, 413 (1994).
[14] J.O. Indekeu, Int. J. Mod. Phys. B **8**, 309 (1994).
[15] L. Leger and J.-F. Joanny, Rep. Prog. Phys. **55**, 431 (1992).
[16] J.G. Dash, H. Fu, and J.S. Wettlaufer, Rep. Prog. Phys. **58**, 115 (1995).
[17] D. Beaglehole and D. Nason, Surf. Sci. **96**, 357 (1980).
[18] Y. Furukawa, J. Cryst. Growth **82**, 665 (1987).
[19] A. Lied, H. Dosch, and J.H. Bilgram, Phys. Rev. Lett. **72**, 3554 (1993).
[20] M. Elbaum, Phys. Rev. Lett. **67**, 2982 (1991); M. Elbaum and M. Schick, *ibid.* **66**, 1713 (1991); M. Elbaum, S.G. Lipson, and J.G. Dash, J. Cryst. Growth **129**, 491 (1993).
[21] R.R. Gilpin, J. Colloid Interface Sci. **77**, 435 (1980).
[22] S.S. Barer, N.V. Churaev, B.V. Derjaguin, O.A. Kiseleva, and V.D. Sobolev, J. Colloid Interface Sci. **74**, 173 (1980).
[23] L.A. Wilen and J.G. Dash, Phys. Rev. Lett. **74**, 5076 (1995). The corresponding theory is developed by J.S. Wettlaufer and M.G. Worster, Phys. Rev. E **51**, 4679 (1995).
[24] Y. Furukawa and I. Ishikawa, J. Cryst. Growth **128**, 1137 (1993).
[25] D. Beaglehole and P. Wilson, J. Phys. Chem. **98**, 8096 (1994).
[26] S. Dietrich and M. Napiórkowski, Phys. Rev. A **43**, 1861 (1991); M. Napiórkowski and S. Dietrich, Phys. Rev. E **47**, 1836 (1993). For a review see S. Dietrich, Phys. Scr. **T49**, 519 (1993).
[27] Equation (2) corresponds to the so-called sharp-kink approximation, where the density is constant in the two coexisting phases and changes abruptly at the interface. The effect of continuously varying density profiles including pronounced density oscillations that are expected close to the wall, as well as of fluctuations of the interfacial configurations might play a role at finite separations, which are considered in this paper [28]. The present theory thus serves as a starting point for a more complete investigation of these additional complications.
[28] For a recent review of fluctuation effects in wetting, see M.E. Fisher, A.J. Jin, and A.O. Parry, Ber. Bunsenges. Phys. Chem. **98**, 357 (1994) and references therein.
[29] The finite value of $P^0(l)$ at vanishing separation is nontrivial and can be derived rigorously using density-functional theory for the calculation of the effective interface potential $P^0(l)$ [26], even though the pair interactions $U_{ij}(\mathbf{r})$ between the dif-

ferent molecules diverge at zero separation.

[30] In the case of volatile liquids, i.e., liquids that are in equilibrium with either the vapor or solid phase, the true interfacial tension between the substrate and the top phase is never larger than the sum of the two tensions γ and γ_{SL} (Antonov's rule), since a liquid layer would always form spontaneously; in fact, the interfacial tension between the third phase and the bare substrate cannot even be measured if the spreading coefficient S, as defined by Eq. (4), is positive. Hence the measurable spreading coefficient is always negative.

[31] F. Brochard-Wyart, J.-M. di Meglio, D. Quéré, and P.-G. de Gennes, Langmuir **7**, 335 (1991).

[32] Experimentally, glass substrates can be roughened by exposing them to HF–Nitric acid, where the surface height fluctuations are determined by the etching time [25].

[33] Here one neglects curvature effects that to leading order, are proportional to $[\nabla^2\zeta_S(\boldsymbol{\rho})]^2$. This approximation is permitted if the substrate corrugation is dominated by small wave numbers; see [34]. The curvature correction for various molecular interactions is calculated in the Appendix.

[34] In the experiment demonstrating roughness-induced interfacial premelting of ice [25], the characteristic height fluctuations have amplitudes and wave numbers in the range of $h_S \approx 2$ nm and $q \approx 0.01\text{nm}^{-1}$, leading to $h_S q \approx 0.02$.

[35] L.A. Wilen, J.S. Wettlaufer, M. Elbaum, and M. Schick, Phys. Rev. B **52**, 12 426 (1995).

[36] J.G. Dash, Phys. Rev. B **25**, 508 (1982).

[37] S. Dietrich (private communication).

[38] J.L. Harden and R.F. Kayser, J. Colloid Interface Sci. **127**, 548 (1989).